Ceramics International xxx (xxxx) xxx–xxx

Contents lists available at ScienceDirect

Ceramics International

journal homepage: www.elsevier.com/locate/ceramint

Microstructure, hardness and fracture toughness of spark plasma sintered ZrB_2–SiC–C_f composites

Mehdi Shahedi Asl

Department of Mechanical Engineering, University of Mohaghegh Ardabili, Ardabil, Iran

ARTICLE INFO

Keywords:
ZrB_2–SiC composite
Carbon fiber
Nano-particles
Taguchi method
Mechanical properties

ABSTRACT

The combined effects of SiC particles and chopped carbon fibers (C_f) as well as sintering conditions on the microstructure and mechanical properties of spark plasma sintered ZrB_2-based composites were investigated by Taguchi methodology. Analysis of variance was used to optimize the spark plasma sintering variables (temperature, time and pressure) and the composition (SiC/C_f ratio) in order to enhance the hardness of ZrB_2–SiC–C_f composites. The sintering temperature was found as the most effective variable, with a significance of 83%, on the hardness. The hardest ZrB_2-based ceramic was achievable by adding 20 vol% SiC and 10 vol% C_f after spark plasma sintering at 1850 °C for 6 min under 30 MPa. Fracture toughness improvement were related to the simultaneous presence of SiC and C_f phases as well as the in-situ formation of nano-sized interfacial ZrC particles. Crack deflection, crack branching and crack bridging were detected as the toughening mechanisms. A Vickers hardness of 14.8 GPa and an indentation fracture toughness of 6.8 MPa $m^{1/2}$ were measured for the sample fabricated at optimal processing conditions.

1. Introduction

Zirconium diboride belongs to a group of ceramic materials with exceedingly high melting point which defines as ultrahigh temperature ceramics (UHTCs) [1–5]. ZrB_2 is an attractive candidate for aerospace applications due to its distinctive combinations of thermomechanical properties such as high electrical and thermal conductivity, high hardness, good thermal shock resistance and high elastic modulus as well as chemical inertness and good dimensional stability [6–9]. However, low fracture toughness and poor oxidation resistance are its serious disadvantages. Sintering process of ZrB_2 is also difficult due to the presence of oxide impurities on the surface of starting particles, the covalent nature of its bonding and low lattice and grain boundary diffusion rates [10–14].

The addition of secondary phases as reinforcement or dopant materials has been identified as effective tactics to improve the mechanical properties of ZrB_2. The effects of different additives such as B_4C [15,16], ZrO_2 [17,18] and ZrC [19,20] on fracture toughness were comprehensively investigated, but among them, ZrB_2–SiC system was recognized to have improved strength and fracture toughness [21–23]. Addition of SiC not only enhances the thermomechanical properties of ZrB_2-based UHTCs, but also increases the oxidation resistance and hinders the abnormal grain growth [24]. Carbonaceous materials in the form of carbon black [25,26], graphite [27–31], carbon nanotube [32–34] and graphene [35,36] were also added to ZrB_2–SiC ceramics to boost their sinterability and mechanical properties.

Carbon fiber is an excellent additive to overcome the low fracture toughness and thermal shock resistance of ZrB_2-based UHTCs on account of its high strength, stiffness and high-temperature endurance [37–41]. It was incorporated into the ZrB_2 matrix by heaterless chemical vapor infiltration to fabricate ZrB_2–SiC ceramic [42,43] and remarkably enhanced the fracture toughness [44]. Prosperous fabrication of hot pressed and spark plasma sintered ZrB_2–SiC ceramics by the addition of carbon fibers as reinforcement material has been recently reported [45]. The fracture toughness of hot pressed 20 vol% carbon fiber reinforced ZrB_2–SiC composite showed an enhancement up to 6.6 MPa $m^{1/2}$, by means of fiber debonding, pull-out and bridging mechanisms [46]. Other toughening mechanisms such as crack deflection and crack branching were also detected in these UHTCs, because of the relatively weak interfacial carbon fiber/matrix bonding [45,47]. However, the flexural strength slightly decreased due to the lower modulus of carbon fiber and the graphitized transition layer between fiber and ZrB_2 matrix [46]. Taguchi methodology was used to determine the most significant additives and spark plasma sintering parameters as well as to optimize the fracture toughness of ZrB_2–SiC composites [48]. By incorporation of carbon fiber in hot pressed ZrB_2–SiC ceramics using nano-sized ZrB_2 powders, a fracture toughness of 6.1 MPa $m^{1/2}$ with non-brittle fracture feature was achieved [49].

The goal of this study is to investigate the microstructure and identify the most important processing variables affecting the hardness of ZrB_2–SiC–C_f composites. The signal to noise ratio (S/N) and the

E-mail address: shahedi@uma.ac.ir.

http://dx.doi.org/10.1016/j.ceramint.2017.08.030
Received 20 July 2017; Received in revised form 3 August 2017; Accepted 3 August 2017
0272-8842/ © 2017 Elsevier Ltd and Techna Group S.r.l. All rights reserved.

Table 1
Conditions for processing of nine composite samples using an L9 orthogonal array.

Sample	Processing variables			
	Temperature (°C)	Dwell time (min)	Pressure (MPa)	vol% SiC/ vol% C_f
1	1650	3	10	4
2	1650	6	20	2
3	1650	9	30	1
4	1750	3	20	1
5	1750	6	30	4
6	1750	9	10	2
7	1850	3	30	2
8	1850	6	10	1
9	1850	9	20	4

analysis of variance (ANOVA) are employed to evaluate the significances and contributions of processing variables on the Vickers hardness. The fracture toughness and toughening mechanisms of the sample fabricated at optimal processing conditions are also discussed.

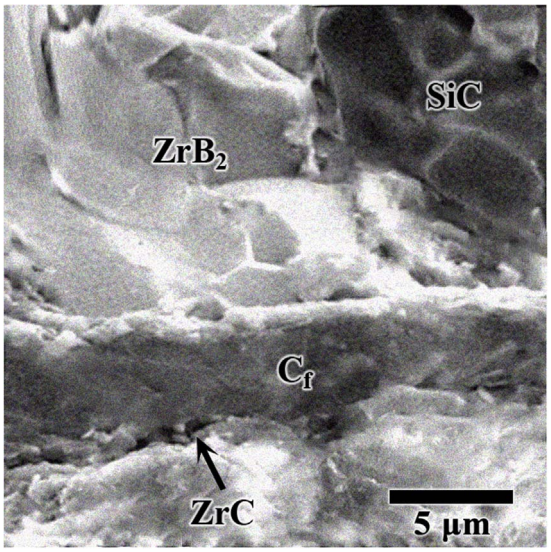

Fig. 2. SEM fractograph of sample 9.

2. Experimental procedure

2.1. Design of experiment

As four processing variables (the spark plasma sintering temperature, time and pressure as well as the composition of samples) have been studied in this research, the design of experiments was conducted by the Taguchi method and L9 orthogonal arrays. Different ratios of SiC and C_f were selected as one of the processing variables, previously called composition. Although C_f has a negative effect on the hardness, because of its softness, however, it was used as an additive due to its beneficially roles on the sinterability and toughening of the ceramic matrix composites. The processing variables, the selected levels and also the nine combinations of variables are presented in Table 1.

Achieving a harder ceramic composite is requested in this research work. Therefore, the statistical analysis is carried out using the "*higher is better*" option to study the output characteristics. Hence, the appropriate formula for determination of S/N ratios is [52,53]:

$$\frac{S}{N} = -10\log\left(\frac{1}{n}\sum_{i=1}^{n}\frac{1}{y_i^2}\right) \quad (1)$$

where y_i (i = 1, 2 ...n) are the response values and n is the number of repetitions. Moreover, the ANOVA analysis is carried out using Qualitek-4 software (Automatic design and analysis of Taguchi experiments, Nutek Inc., Michigan, USA) to evaluate the significances and contributions of processing variables on the hardness of ZrB_2–SiC–C_f composites.

Table 2
Experimental values and corresponding S/N ratios for Vickers hardness of spark plasma sintered ZrB_2-based composites.

Sample	Vickers hardness (GPa)						S/N ratio
	Trial 1	Trial 2	Trial 3	Trial 4	Trial 5	Average	
1	7.0	6.4	6.1	5.5	6.6	6.3	15.9
2	8.9	8.8	9.0	8.5	9.1	8.9	18.9
3	8.8	8.1	8.9	8.0	9.1	8.6	18.6
4	9.3	9.2	9.1	9.4	8.8	9.2	19.2
5	10.8	10.5	10.2	10.0	11.2	10.5	20.4
6	9.7	10.5	10.2	10.5	11.0	10.4	20.3
7	14.0	14.9	15.2	13.2	13.7	14.2	23.0
8	13.6	14.6	12.9	12.8	13.9	13.6	22.6
9	12.5	12.8	12.9	11.9	13.4	12.7	22.0
Grand average					10.5	20.1	

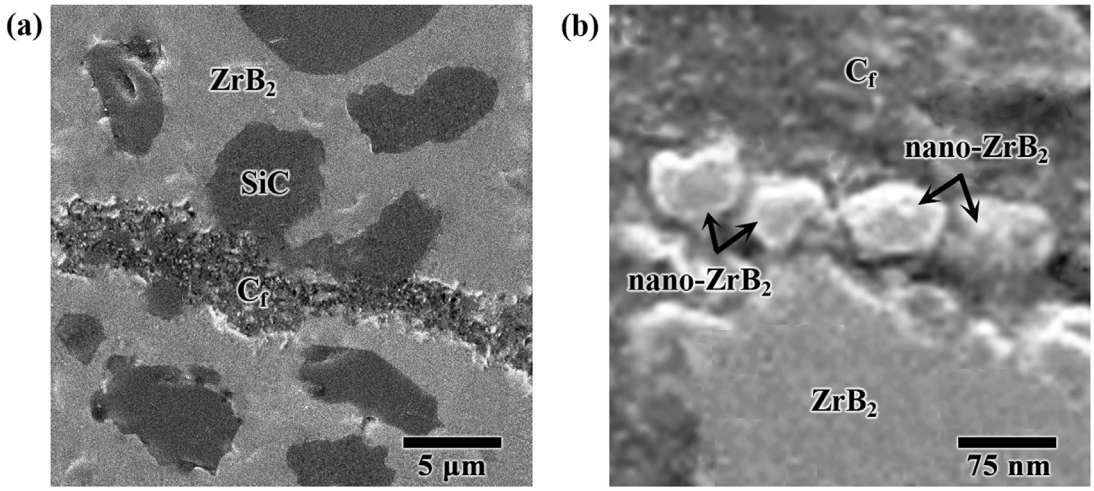

Fig. 1. (a) SEM micrograph of the polished surface of sample 8 and (b) a closer view of C_f/ZrB_2 interface in figure a showing the in-situ formation of nano-sized ZrB_2 particles.

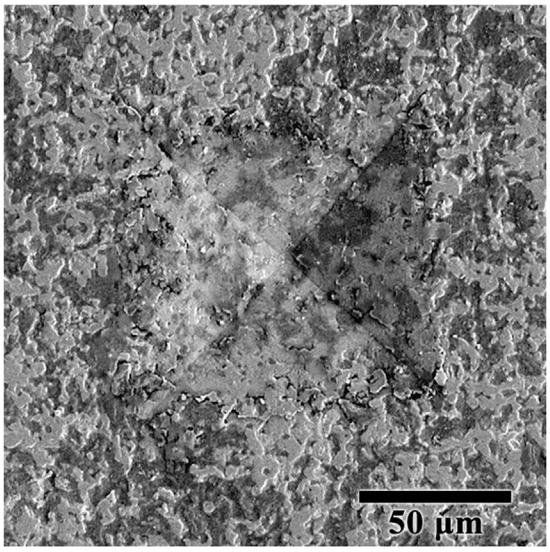

Fig. 3. SEM micrograph of the Vickers indenter's impression on the polished surface of sample 2.

2.2. Materials and process

Commercial ZrB_2 powder (particle size: 1–3 µm, purity: 99.9%, Xuzhou Hongwu Co., China), SiC powder (particle size: 1–10 µm, purity: 99%, Xuzhou Hongwu Co., China) and chopped carbon fiber (length: 1–3 mm, diameter: 5 µm, Torayca Sigmatex Ltd, United Kingdom) were used as starting materials. Three pellets, with a diameter of 24 mm and thickness of ~ 6 mm, were prepared for each condition. In this way, three distinctive mixtures were prepared as ZrB_2–24 vol% SiC–6 vol% C_f, ZrB_2–20 vol% SiC–10 vol% C_f and ZrB_2–15 vol% SiC–15 vol% C_f in order to supply the desired SiC/ C_f ratios of 4, 2 and 1, respectively. At the beginning, the chopped carbon fibers were dispersed ultrasonically for 20 min in ethanol. The ZrB_2 and SiC powders were then added to the slurry and ball-mixed in a zirconia cup for 20 min using zirconia balls. The wet mixtures were subsequently dried at 120 °C for 48 h on a rotating drier. Eventually, the powders were loaded into a graphite die and the spark plasma sintering process was performed in a SPS hot pressing furnace (SPS-20T-10, China) in vacuum atmosphere. The sintering processes were accomplished at the temperature of 1650, 1750 or 1850 °C, for the dwell time of 3, 6 or 9 min under the pressure of 10, 20 or 30 MPa, according to Table 1. Finally, the furnace was cooled down and the sintered pellets were removed.

2.3. Characterization

Field emission scanning electron microscopy (FESEM: Sigma/VP, Zeiss) was used for microstructural investigations, equipped with energy dispersive spectroscopy for chemical analysis. Hardness (HV5.0) of the samples was determined by Vickers indentation (Zwick Roell ZHV 10, Germany) on the polished surfaces, prepared by mechanical polishing to 1-µm quality, using a load of 5 kg and a dwell time of 15 s. Reported hardness values were obtained from the average of five measurements. The elastic moduli were approximated using the following equation [54]:

$$E = E_0 \frac{(1-P)^2}{1+\frac{P}{\rho-1}} \tag{2}$$

where E_0 is the modulus of a hypothetical fully dense sample estimated by the rule of mixtures, P is the vol% of porosity and ρ is the Nielsen shape factor (0.4). Elastic modulus of ZrB_2, SiC and C_f were considered as 500, 410 and 230 GPa, respectively. The indentation fracture toughness (K_{IC}) was determined from the lengths of the indentation-induced cracks using the Anstis formula [55]:

$$K_{1C} = (0.016 \pm 0.004)\left(\frac{E}{H_V}\right)^{1/2} \frac{L}{c^{3/2}} \tag{3}$$

where E is the elastic modulus, H_V is the value of Vickers hardness, L is the indentation load, and c is the half of mean length of radial cracks.

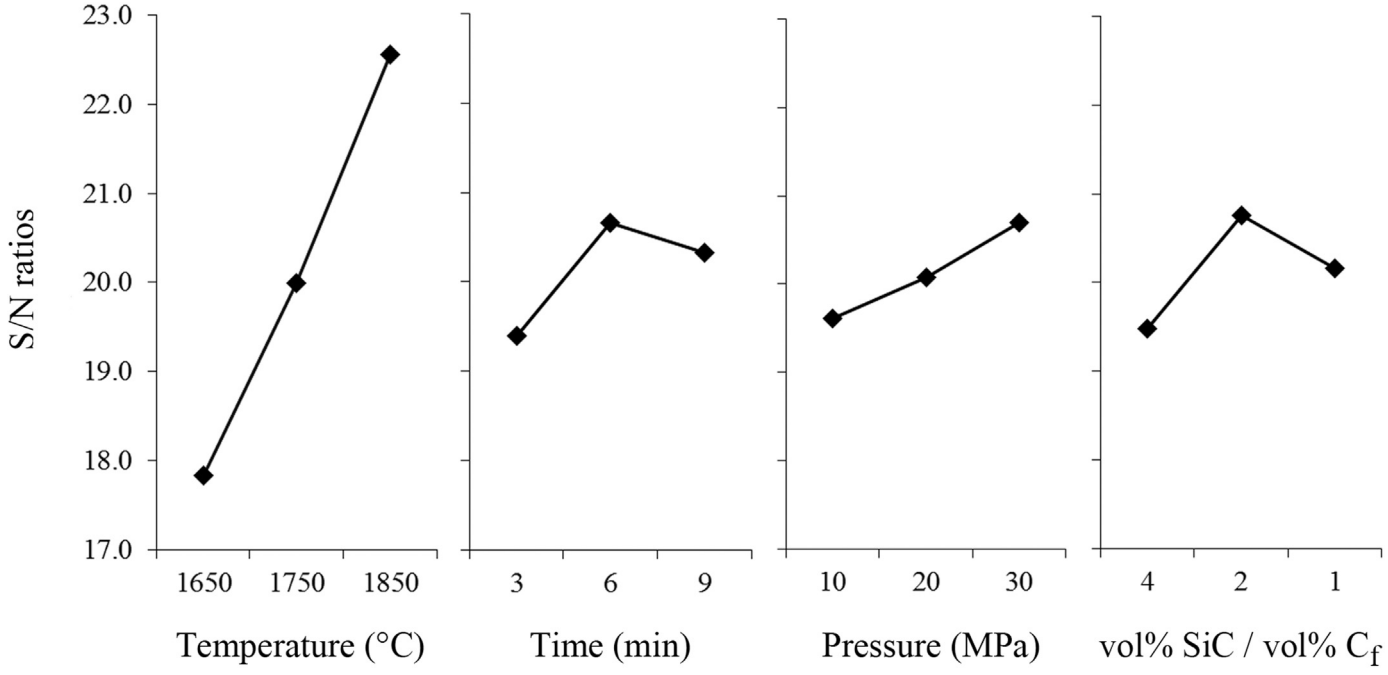

Fig. 4. S/N ratios of the processing variables for the Vickers hardness.

Table 3
ANOVA results explaining the significances of processing variables on Vickers hardness of ZrB_2-based composites.

Process parameters	Degrees of freedom (f)	Sum of squares (S)	Variance (V)	Pure sum (S′)	Significance P (%)
Temperature	2	33.6	16.8	33.6	83.1
Dwell time	2	2.6	1.3	2.6	6.5
Pressure	2	1.8	0.9	1.8	4.3
Composition	2	2.5	1.2	2.5	6.1
Total	8	40.4	–	–	100.0

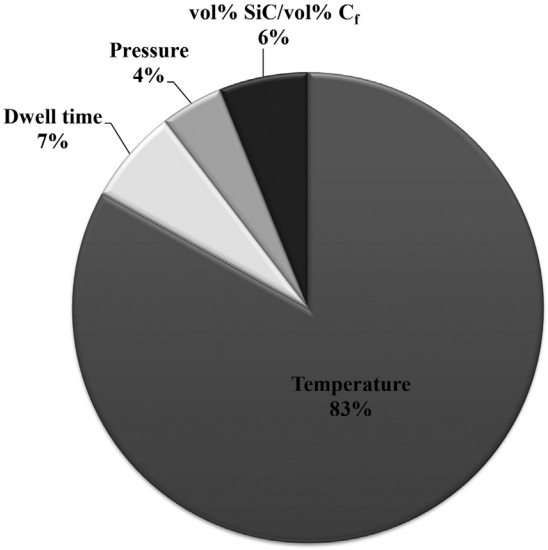

Fig. 5. Significance of processing variables on the Vickers hardness of ZrB_2-based composite.

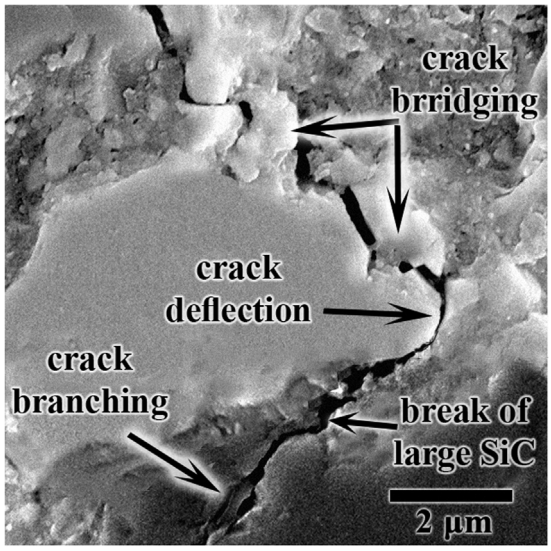

Fig. 6. SEM micrograph of the indentation-induced crack path showing the toughening mechanisms in the sample sintered at optimal conditions.

Table 4
Optimum conditions and performance for the Vickers hardness of ZrB_2-based composites.

Factor	Level description	Level	Contribution (GPa)
Temperature (°C)	1850	3	3.0
Dwell time (min)	6	2	0.5
Pressure (MPa)	30	3	0.6
vol% SiC/vol% C_f	2	2	0.7
Total contribution of all factors			4.8
Current grand average of performance			10.5
Expected result at optimum conditions			15.3
Experimented result at optimal processing conditions			14.8 ± 3.2

3. Results and discussion

3.1. Microstructure and sinterability

In the literature, it was reported that the surface oxide impurities of initial ZrB_2 powders (i.e. ZrO_2 and B_2O_3) resulted in grain coarsening and hindered the sintering process [50,51]. The hot pressing temperature was recognized as the most effective variable on densification behavior and microstructure of ZrB_2–SiC–C_f UHTCs [50]. Carbon reacts with such interloper oxides and removes them as a sintering aid in ZrB_2–SiC composites. The occurrence of such carbothermal chemical reaction can be clearly seen in the SEM image of polished surface of sample 8 (Fig. 1a). The reduction of oxide impurities to the nano-sized ZrB_2 particles at the interfaces of C_f and initial ZrB_2 powder is also observed in the SEM nanograph of Fig. 1b.

The previously reported thermodynamical and microstructural assessments [50] verified the formation of ZrC phase in hot pressed ZrB_2–SiC–C_f composites. Such in-situ formed interfacial phase is also shown in the SEM fractograph of sample 9, marked by arrow in Fig. 2.

The simultaneous presence of SiC, C_f and ZrC as the reinforcement phases in ZrB_2-based composites was found to have important effects on the densification, grain growth, and generally, on the sintering process and microstructure evolution.

3.2. Hardness analysis

The outcomes of hardness measurements and corresponding S/N ratios are presented in Table 2. The results confirmed that the hardness shows a wide variation within the range of processing variables investigated in this research. Vickers hardness increased from 6.3 GPa for sample 1 with a relative density of ~ 82% to 14.2 GPa when the relative density reached ~ 100% (sample 7). Hence, it can be clearly found that the relative density controls the hardness. As the concept of hardness is how a material can resist against the plastic deformation, due to the applied compressive force [4], a more porous sample shows less resistance against the Vickers indentation load. Fig. 3 shows the scanning electron microscopy image of the Vickers indenter's impression on the polished surface of sample 2, which was spark plasma sintered at 1650 °C for 6 min under 20 MPa with SiC/C_f ratio of 2.

The main effect plots for Vickers hardness, exhibiting the changes in S/N ratios with processing variables, are exhibited in Fig. 4. A very sharp and a mild increase in the S/N ratios are obviously seen in these plots with raising the sintering temperature and applied pressure, respectively. With increasing the dwell time or SiC/C_f ratio, a mild increase and then a slighter decrease in the S/N ratios are observed. Generally, the hardness of composite enhances with increasing the spark plasma sintering conditions (temperature, dwell time and applied pressure). Moreover, from the viewpoint of composition of UHTC, the maximum S/N ratio for the Vickers hardness corresponds to the SiC/C_f ratio of 2. Therefore, the highest value of Vickers hardness is obtainable for ZrB_2–20 vol% SiC–10 vol% C_f composite by spark plasma sintering at 1850 °C for 6 min under 30 MPa.

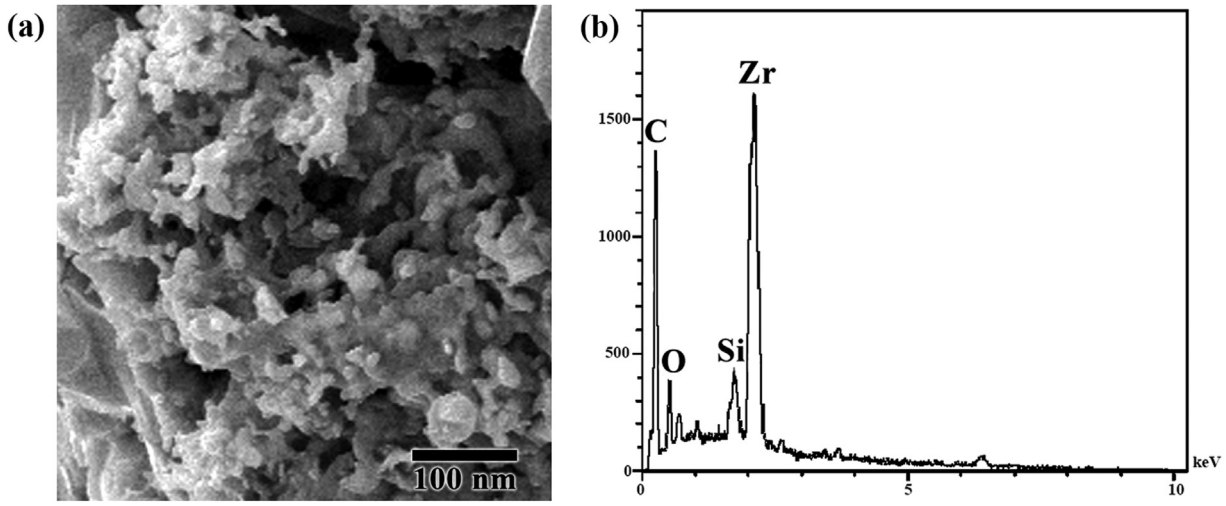

Fig. 7. (a) SEM nanograph of the in-situ formed ZrC at ZrB_2/C_f interface and (b) corresponding EDS spectrum of such ZrC nano-particles.

The ANOVA results of significance of processing parameters on the Vickers hardness are presented in Table 3, which identifies the sintering temperature as the most effective variable on the hardness of ZrB_2-based composites. Based on the ANOVA, other processing variables (dwell time, applied pressure and SiC/C_f ratio) had no remarkable influences on the hardness of samples. Fig. 5 summarizes the AVONA results as a significance pie chart of the processing variables on the Vickers hardness. The significances of sintering temperature, dwell time, applied pressure and SiC/C_f ratio are calculated ~ 83%, ~ 7%, ~ 4% and ~ 6%, respectively.

The performance and contribution of processing variables for Vickers hardness at the optimal conditions is outlined in Table 4. At such processing conditions (the temperature of 1850 °C, the dwell time of 6 min, the pressure of 30 MPa and the SiC/C_f ratio of 2), the hardness can reach the maximum value. The grand average of performance for the hardness values of nine experiments is estimated as 10.5 GPa (Table 2). In addition, the contributions of sintering temperature, dwell time, applied pressure and SiC/C_f ratio on the Vickers hardness enhancement at such optimal conditions are 3.0, 0.5, 0.6, and 0.7 GPa, respectively; hence, the total contributions of all factors are 4.8 GPa. Consequently, the expected hardness value at the optimal conditions is 15.3 GPa. In order to check the validity of ANOVA prognostication, a confirmation test at the actual optimal conditions is needed. A hardness of 14.8 GPa was experimentally achieved as the result of confirmation test, which is very close to the predicted value by ANOVA. Therefore, the efficacy of Taguchi design of experiments and ANOVA methodology for optimization of processing variables to reach the hardest ZrB_2–SiC–C_f composite is ascertained.

3.3. Fracture toughness

In this study, due to the significant amounts of porosities presented in the polished surfaces of porous ceramics, the indentation-induced cracks are not observable in all samples. Hence, as a result of interactions between the pores and cracks in the porous samples, the indentation method is not reliable for the fracture toughness evaluation. Therefore, ANOVA estimations and predictions are meaningless in this case. Thus, the indentation technique was employed only for the sample sintered at optimal conditions and a fracture toughness value of 6.8 MPa $m^{1/2}$ was calculated. The SEM micrograph of crack propagating path, induced by the Vickers indenter, is presented in Fig. 6. The indentation crack path obviously exhibits several toughening mechanisms such as crack bridging, crack deflection, crack branching and break of large SiC particle. These mechanisms, as also reported in ZrB_2-based ceramics reinforced/doped with other carbonaceous materials [26,28,33,35], result in the dissipation of crack's energy and consequently fracture toughness enhancement.

The improvement in the fracture toughness of this sample can also be related to the in-situ formation of ZrC phase at the interfaces of ZrB_2 and C_f. Fig. 7a shows the SEM nanograph of such in-situ formed ZrC nano-particles at ZrB_2/C_f interface (closer view of the marked area in Fig. 2). EDS spectrum of such nano-sized interfacial phases (Fig. 7a), implies the presence of high amount zirconium and carbon elements as a sign of ZrC formation. During the cooling step, the differences in thermal expansion coefficients of constituents (ZrB_2: 5.9–6.8 × 10^{-6} K^{-1}, SiC: 4–4.7 × 10^{-6} K^{-1}, graphite: 0.5 × 10^{-6} K^{-1} for a-axis/ 30 × 10^{-6} K^{-1} for c-axis and ZrC: 4.7–7.1 × 10^{-6} K^{-1}) [18,28] lead to the generation of residual stresses at the interfaces of constituents. As a result of the thermal expansion mismatch between these phases, it seems that other toughening mechanisms such as microcracking are also feasible.

4. Conclusions

The effects of spark plasma sintering variables (sintering temperature, dwell time and applied pressure) and composition (SiC/C_f ratio) on microstructure, sinterability and mechanical properties of ZrB_2–SiC–C_f composites were investigated by Taguchi methodology and analysis of variance. The sintering temperature was revealed as the most effective variable on the hardness with a significance of 83%. The temperature of 1850 °C, the dwell time of 6 min, the pressure of 30 MPa and the SiC/C_f ratio of 2 were determined as the optimal processing conditions. A ZrB_2–20 vol% SiC–10 vol% C_f composite with a hardness of 14.8 GPa and a fracture toughness of 6.8 MPa $m^{1/2}$ was obtained at the optimum sintering conditions. The activation of several toughening mechanisms such as crack deflection, crack branching, crack bridging and microcracking were attributed to the combined influences of SiC, C_f and in-situ formed ZrC nano-particles.

Acknowledgment

The author would like to thank the Arta Research Group (www.artaresearch.com) for its financial support through Grant ARG-2500-002.

References

[1] M. Shahedi Asl, M. Ghassemi Kakroudi, B. Nayebi, H. Nasiri, Taguchi analysis on the effect of hot pressing parameters on density and hardness of zirconium diboride, Int. J. Refract. Met. Hard Mater. 50 (2015) 313–320.
[2] M. Shahedi Asl, M. Ghassemi Kakroudi, A processing–microstructure correlation in

ZrB_2–SiC composites hot-pressed under a load of 10 MPa, Univers. J. Mater. Sci. 3 (2015) 14–21.
[3] K. Farhadi, A. Sabahi Namini, M. Shahedi Asl, A. Mohammadzadeh, M. Ghassemi Kakroudi, Characterization of hot pressed SiC whisker reinforced TiB2 based composites, Int. J. Refract. Met. Hard Mater. 61 (2016) 84–90.
[4] M. Shahedi Asl, Z. Ahmadi, S. Parvizi, Z. Balak, I. Farahbakhsh, Contribution of SiC particle size and spark plasma sintering conditions on grain growth and hardness of TiB_2 composites, Ceram. Int. (2017). http://dx.doi.org/10.1016/j.ceramint.2017.07.121.
[5] A. Sabahi Namini, S.N. Seyed Gogani, M. Shahedi Asl, K. Farhadi, M. Ghassemi Kakroudi, A. Mohammadzadeh, Microstructural development and mechanical properties of hot pressed SiC reinforced TiB_2 based composite, Int. J. Refract. Met. Hard Mater. 51 (2015) 169–179.
[6] Z. Ahmadi, B. Nayebi, M. Shahedi Asl, M. Ghassemi Kakroudi, I. Farahbakhsh, Sintering behavior of ZrB_2–SiC composites doped with Si_3N_4: A fractographical approach, Ceram. Int. 43 (2017) 9699–9708.
[7] M. Jaberi Zamharir, M. Shahedi Asl, M. Ghassemi Kakroudi, N. Pourmohammadie Vafa, M. Jaberi Zamharir, "Significance of hot pressing parameters and reinforcement size on sinterability and mechanical properties of ZrB_2–25 vol% SiC UHTCs, Ceram. Int. 41 (2015) 9628–9636.
[8] M. Shahedi Asl, M. Ghassemi Kakroudi, M. Rezvani, F. Golestani-Fard, Significance of hot pressing parameters on the microstructure and densification behavior of zirconium diboride, Int. J. Refract. Met. Hard Mater. 50 (2015) 140–145.
[9] M. Jaberi Zamharir, M. Shahedi Asl, N. Pourmohammadie Vafa, M. Ghassemi Kakroudi, Significance of hot pressing parameters and reinforcement size on densification behavior of ZrB_2–25 vol% SiC UHTCs, Ceram. Int. 41 (2015) 6439–6447.
[10] Z. Balak, M. Azizieh, H. Kafashan, M. Shahedi Asl, Z. Ahmadi, Optimization of effective parameters on thermal shock resistance of ZrB_2-SiC-based composites prepared by SPS: using Taguchi design, Mater. Chem. Phys. 196 (2017) 333–340.
[11] M. Shahedi Asl, B. Nayebi, Z. Ahmadi, P. Pirmohammadi, M. Ghassemi Kakroudi, Fractographical characterization of hot pressed and pressureless sintered SiAlON-doped ZrB_2–SiC composites, Mater. Charact. 102 (2015) 137–145.
[12] M. Shahedi Asl, M. Ghassemi Kakroudi, Fractographical Assessment of densification mechanisms in hot pressed ZrB_2-SiC composites, Ceram. Int. 40 (2014) 15273–15281.
[13] M. Shahedi Asl, M. Ghassemi Kakroudi, A. Farzaneh, B. Nayebi, Influence of nano-SiC participation on densification and mechanical properties of ZrB_2, in: Proceedings of the 10th Nanoscience and Nanotechnology Conference of Turkey (NanoTR10), Istanbul, 2014.
[14] Z. Ahmadi, B. Nayebi, M. Shahedi Asl, M. Ghassemi Kakroudi, Fractographical characterization of hot pressed and pressureless sintered AlN-doped ZrB_2–SiC composites, Mater. Charact. 110 (2015) 77–85.
[15] B. Nayebi, M. Shahedi Asl, M. Ghassemi Kakroudi, I. Farahbakhsh, M. Shokouhimehr, Interfacial phenomena and formation of nano-particles in porous ZrB_2–40 vol% B_4C UHTC, Ceram. Int. 42 (2016) 17009–17015.
[16] M. Shahedi Asl, M. Ghassemi Kakroudi, B. Nayebi, A fractographical approach to the sintering process in porous ZrB_2-B_4C binary composites, Ceram. Int. 41 (2015) 379–387.
[17] N. Pourmohammadie Vafa, M. Shahedi Asl, M. Jaberi Zamharir, M. Ghassemi Kakroudi, Reactive hot pressing of ZrB_2-based composites with changes in ZrO_2/SiC ratio and sintering conditions. Part I: densification behavior, Ceram. Int. 41 (2015) 8388–8396.
[18] N. Pourmohammadie Vafa, B. Nayebi, M. Shahedi Asl, M. Jaberi Zamharir, M. Ghassemi Kakroudi, Reactive hot pressing of ZrB_2-based composites with changes in ZrO_2/SiC ratio and sintering conditions. Part II: mechanical behavior, Ceram. Int. 42 (2016) 2724–2733.
[19] H.L. Liu, G.J. Zhang, J.X. Liu, H. Wu, Synergetic roles of ZrC and SiC in ternary ZrB_2–SiC–ZrC ceramics, J. Eur. Ceram. Soc. 35 (2015) 4389–4397.
[20] H.L. Liu, J.X. Liu, H.T. Liu, G.J. Zhang, Contour maps of mechanical properties in ternary ZrB_2 single bond SiC single bond ZrC ceramic system, Scr. Mater. 107 (2015) 140–144.
[21] M. Shahedi Asl, M. Ghassemi Kakroudi, F. Golestani-Fard, H. Nasiri, A Taguchi approach to the influence of hot pressing parameters and SiC content on the sinterability of ZrB_2-based composites, Int. J. Refract. Met. Hard Mater. 51 (2015) 81–90.
[22] M. Shahedi Asl, M. Ghassemi Kakroudi, S. Noori, Hardness and toughness of hot pressed ZrB_2-SiC composites consolidated under relatively low pressure, J. Alloy. Compd. 619 (2015) 481–487.
[23] M. Shahedi Asl, A. Sabahi Namini, M. Ghassemi Kakroudi, Influence of silicon carbide addition on the microstructural development of hot pressed zirconium and titanium diborides, Ceram. Int. 42 (2016) 5375–5381.
[24] Q. Liu, W. Han, X. Zhang, S. Wang, J. Han, Microstructure and mechanical properties of ZrB_2-SiC composites, Mater. Lett. 63 (2009) 1323–1325.
[25] S. Zhou, Z. Wang, X. Sun, J. Han, Microstructure, mechanical properties and thermal shock resistance of zirconium diboride containing silicon carbide ceramic toughened by carbon black, Mater. Chem. Phys. 122 (2010) 470–473.
[26] I. Farahbakhsh, Z. Ahmadi, M. Shahedi Asl, Densification, microstructure and mechanical properties of hot pressed ZrB_2–SiC ceramic doped with nano-sized carbon black, Ceram. Int. 43 (2017) 8411–8417.
[27] Z. Wang, C. Hong, X. Zhang, X. Sun, J. Han, Microstructure and thermal shock behavior of ZrB_2–SiC–graphite composite, Mater. Chem. Phys. 113 (2009) 338–341.
[28] M. Shahedi Asl, M. Ghassemi Kakroudi, R. Abedi Kondolaji, H. Nasiri, Influence of graphite nano-flakes on densification and mechanical properties of hot-pressed ZrB_2–SiC composite, Ceram. Int. 41 (2015) 5843–5851.
[29] Z. Wang, S. Wang, X. Zhang, P. Hu, W. Han, C. Hong, Effect of graphite flake on microstructure as well as mechanical properties and thermal shock resistance of ZrB_2–SiC matrix ultrahigh temperature ceramics, J. Alloy. Compd. 484 (2009) 390–394.
[30] X. Zhang, Z. Wang, X. Sun, W. Han, C. Hong, Effect of graphite flake on the mechanical properties of hot pressed ZrB_2–SiC ceramics, Mater. Lett. 62 (2008) 4360–4362.
[31] S. Zhou, Z. Wang, W. Zhang, Effect of graphite flake orientation on microstructure and mechanical properties of ZrB_2–SiC–graphite composite, J. Alloy. Compd. 485 (2009) 181–185.
[32] G.B. Yadhukulakrishnan, A. Rahman, S. Karumuri, M.M. Stackpoole, A.K. Kalkan, R.P. Singh, S.P. Harimkar, Spark plasma sintering of silicon carbide and multi-walled carbon nanotube reinforced zirconium diboride ceramic composite, Mater. Sci. Eng. A 552 (2012) 125–133.
[33] M. Shahedi Asl, I. Farahbakhsh, B. Nayebi, Characteristics of multi-walled carbon nanotube toughened ZrB_2–SiC ceramic composite prepared by hot pressing, Ceram. Int. 42 (2016) 1950–1958.
[34] W.B. Tian, Y.M. Kan, G.J. Zhang, P.L. Wang, Effect of carbon nanotubes on the properties of ZrB_2–SiC ceramics, Mater. Sci. Eng. A 487 (2008) 568–573.
[35] M. Shahedi Asl, M. Ghassemi Kakroudi, Characterization of hot-pressed graphene reinforced ZrB_2–SiC composite, Mater. Sci. Eng. A 625 (2015) 385–392.
[36] G.B. Yadhukulakrishnan, S. Karumuri, A. Rahman, R.P. Singh, A.K. Kalkan, S.P. Harimkar, Spark plasma sintering of graphene reinforced zirconium diboride ultra-high temperature ceramic composites, Ceram. Int. 39 (2013) 6637–6646.
[37] F. Yang, X. Zhang, J. Han, S. Du, Mechanical properties of short carbon fiber reinforced ZrB_2–SiC ceramic matrix composites, Mater. Lett. 62 (2008) 2925–2927.
[38] D.B. Marshall, A.G. Evans, Failure mechanisms in ceramic-fiber/ceramic-matrix composites, J. Am. Ceram. Soc. 68 (1985) 225–231.
[39] J. Liu, Z. Yue, H. Fong, Continuous nanoscale carbon fibers with superior mechanical strength, Small 5 (2009) 536–542.
[40] R. Tressler, Recent developments in fibers and interphases for high temperature ceramic matrix composites, Compos. Part A Appl. Sci. Manuf. 30 (1999) 429–437.
[41] F. Yang, X. Zhang, J. Han, S. Du, Processing and mechanical properties of short carbon fibers toughened zirconium diboride-based ceramics, Mater. Des. 29 (2008) 1817–1820.
[42] B. Nayebi, M. Shahedi Asl, M. Ghassemi Kakroudi, M. Shokouhimehr, Temperature dependence of microstructure evolution during hot pressing of ZrB_2–30 vol% SiC composites, Int. J. Refract. Met. Hard Mater. 54 (2016) 7–13.
[43] S. Tang, J. Deng, S. Wang, W. Liu, Fabrication and characterization of an ultra-high-temperature carbon fiber-reinforced ZrB_2-SiC matrix composite, J. Am. Ceram. Soc. 90 (2007) 3320–3322.
[44] S. Tang, J. Deng, S. Wang, W. Liu, Fabrication and characterization of C/SiC composites with large thickness, high density and near-stoichiometric matrix by heaterless chemical vapor infiltration, Mater. Sci. Eng. A 465 (2007) 290–294.
[45] K. Gui, P. Hu, W. Hong, X. Zhang, S. Dong, Microstructure, mechanical properties and thermal shock resistance of ZrB_2-SiC-C_f composite with inhibited degradation of carbon fibers, J. Alloy. Compd. 706 (2017) 16–23.
[46] F. Yang, X. Zhang, J. Han, S. Du, Characterization of hot-pressed short carbon fiber reinforced ZrB_2-SiC ultra-high temperature ceramic composites, J. Alloy. Compd. 472 (2009) 395–399.
[47] D. Taylor, P. Cornetti, N. Pugno, The fracture mechanics of finite crack extension, Eng. Fract. Mech. 72 (2005) 1021–1038.
[48] Z. Balak, M. Shahedi Asl, M. Azizieh, H. Kafashan, R. Hayati, Effect of different additives and open porosity on fracture toughness of ZrB_2–SiC-based composites prepared by SPS, Ceram. Int. 43 (2017) 2209–2220.
[49] P. Hu, K. Gui, W. Hong, X. Zhang, S. Dong, High-performance ZrB_2-SiC-C_f composite prepared by low-temperature hot pressing using nanosized ZrB_2 powder, J. Eur. Ceram. Soc. 37 (2017) 2317–2324.
[50] M. Shahedi Asl, F. Golmohammadi, M. Ghassemi Kakroudi, M. Shokouhimehr, Synergetic effects of SiC and C_{sf} in ZrB_2-based ceramic composites. Part I: densification behavior, Ceram. Int. 42 (2016) 4498–4506.
[51] M. Shahedi Asl, M. Ghassemi Kakroudi, I. Farahbakhsh, B. Mazinani, Z. Balak, Synergetic effects of SiC and C_{sf} in ZrB_2-based ceramic composites. Part II: grain growth, Ceram. Int. 42 (2016) 18612–18619.
[52] R. Roy, A Primer on the Taguchi method, Van Nostrand Rheinhold, New York, 1990.
[53] D.C. Montgomery, Introduction to Statistical Quality Control, sixth ed., John Wiley & Sons, Inc, United States of America, 2009.
[54] L.F. Nielsen, Elasticity and damping of porous materials and impregnated materials, J. Am. Ceram. Soc. 67 (2) (1984) 93–98.
[55] G.R. Anstis, P. Chantikul, B.R. Lawn, D.B. Marshall, A critical evaluation of indentation techniques for measuring fracture toughness: I, direct crack measurements, J. Am. Ceram. Soc. 64 (9) (1981) 533–538.